NANO LETTERS

Letter

Graphene-Based Ultracapacitors

Meryl D. Stoller, Sungjin Park, Yanwu Zhu, Jinho An, and Rodney S. Ruoff

Nano Lett., **2008**, 8 (10), 3498-3502 • DOI: 10.1021/nl802558y • Publication Date (Web): 13 September 2008

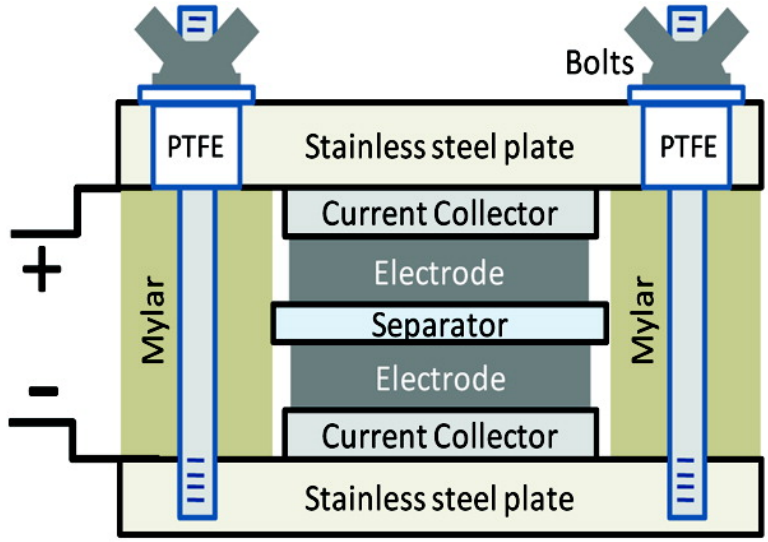

More About This Article

Additional resources and features associated with this article are available within the HTML version:

- Supporting Information
- Access to high resolution figures
- Links to articles and content related to this article
- Copyright permission to reproduce figures and/or text from this article

View the Full Text HTML

NANO LETTERS

2008
Vol. 8, No. 10
3498-3502

Graphene-Based Ultracapacitors

Meryl D. Stoller, Sungjin Park, Yanwu Zhu, Jinho An, and Rodney S. Ruoff*

Department of Mechanical Engineering and Texas Materials Institute, University of Texas at Austin, One University Station C2200, Austin, Texas, 78712-0292

Received August 22, 2008

ABSTRACT

The surface area of a single graphene sheet is 2630 m^2/g, substantially higher than values derived from BET surface area measurements of activated carbons used in current electrochemical double layer capacitors. Our group has pioneered a new carbon material that we call chemically modified graphene (CMG). CMG materials are made from 1-atom thick sheets of carbon, functionalized as needed, and here we demonstrate in an ultracapacitor cell their performance. Specific capacitances of 135 and 99 F/g in aqueous and organic electrolytes, respectively, have been measured. In addition, high electrical conductivity gives these materials consistently good performance over a wide range of voltage scan rates. These encouraging results illustrate the exciting potential for high performance, electrical energy storage devices based on this new class of carbon material.

Ultracapacitors based on electrochemical double layer capacitance (EDLC) are electrical energy storage devices that store and release energy by nanoscopic charge separation at the electrochemical interface between an electrode and an electrolyte.[1] As the energy stored is inversely proportional to the thickness of the double layer, these capacitors have an extremely high energy density compared to conventional dielectric capacitors. They are able to store a large amount of charge which can be delivered at much higher power ratings than rechargeable batteries. An ultracapacitor can be used in a wide range of energy capture and storage applications and are used either by themselves as the primary power source or in combination with batteries or fuel cells. Some advantages of ultracapacitors over more traditional energy storage devices include high power capability, long life, a wide thermal operating range, low weight, flexible packaging, and low maintenance.[2] Ultracapacitors are ideal for any application having a short load cycle and high reliability requirement, such as energy recapture sources including load cranes, forklifts, and electric vehicles.[2,3] Other applications that exploit an ultracapacitor's ability to nearly instantaneously absorb and release power include power leveling for electric utilities and factory power backup. A bank of ultracapacitors, for example, can bridge the short time duration between a power failure and the startup of backup power generators. While the energy density of ultracapacitors is very high compared to conventional dielectric capacitors, it is still significantly lower than batteries or fuel cells. Coupling with batteries (or another power source) is still required for supplying energy for longer periods of time. Thus, there is a strong interest, for example, as enunciated by the U.S. Department of Energy, for increasing the energy density of ultracapacitors to be closer to the energy density of batteries.[4] In addition to the EDLCs (described above), another class of ultracapacitor that is based on pseudocapacitance can be employed. While the charge storage mechanism of EDLCs is nonfaradic, pseudocapacitance is based on faradic, redox reactions using electrode materials such as electrically conducting polymers and metal oxides. The energy densities of pseudocapacitance-based devices can be greater than EDLCs, however, the phase changes within the electrode due to the faradic reaction limits their lifetime and power density. The results reported here are based on EDLC ultracapacitor cells with CMG-based carbon electrode material.

An ultracapacitor unit cell is comprised of two porous carbon electrodes that are isolated from electrical contact by a porous separator.[5] Current collectors of metal foil or carbon impregnated polymers are used to conduct electrical current from each electrode. The separator and the electrodes are impregnated with an electrolyte, which allows ionic current to flow between the electrodes while preventing electronic current from discharging the cell. A packaged ultracapacitor module, depending upon the desired size and voltage, is constructed of multiple repeating unit cells.

The CMG system of individual sheets does not depend on the distribution of pores in a solid support to give it its large surface area, rather every chemically modified graphene sheet can "move" physically to adjust to the different types of electrolytes (their sizes, their spatial distribution). Thus, access to the very high surface area of CMG materials by the electrolyte can be maintained while preserving the overall high electrical conductivity for such a network.[6,7] Because of the relatively high electrical resistance of activated carbon

* To whom correspondence should be addressed. E-mail: r.ruoff@mail.utexas.edu.

10.1021/nl802558y CCC: $40.75
Published on Web 09/13/2008

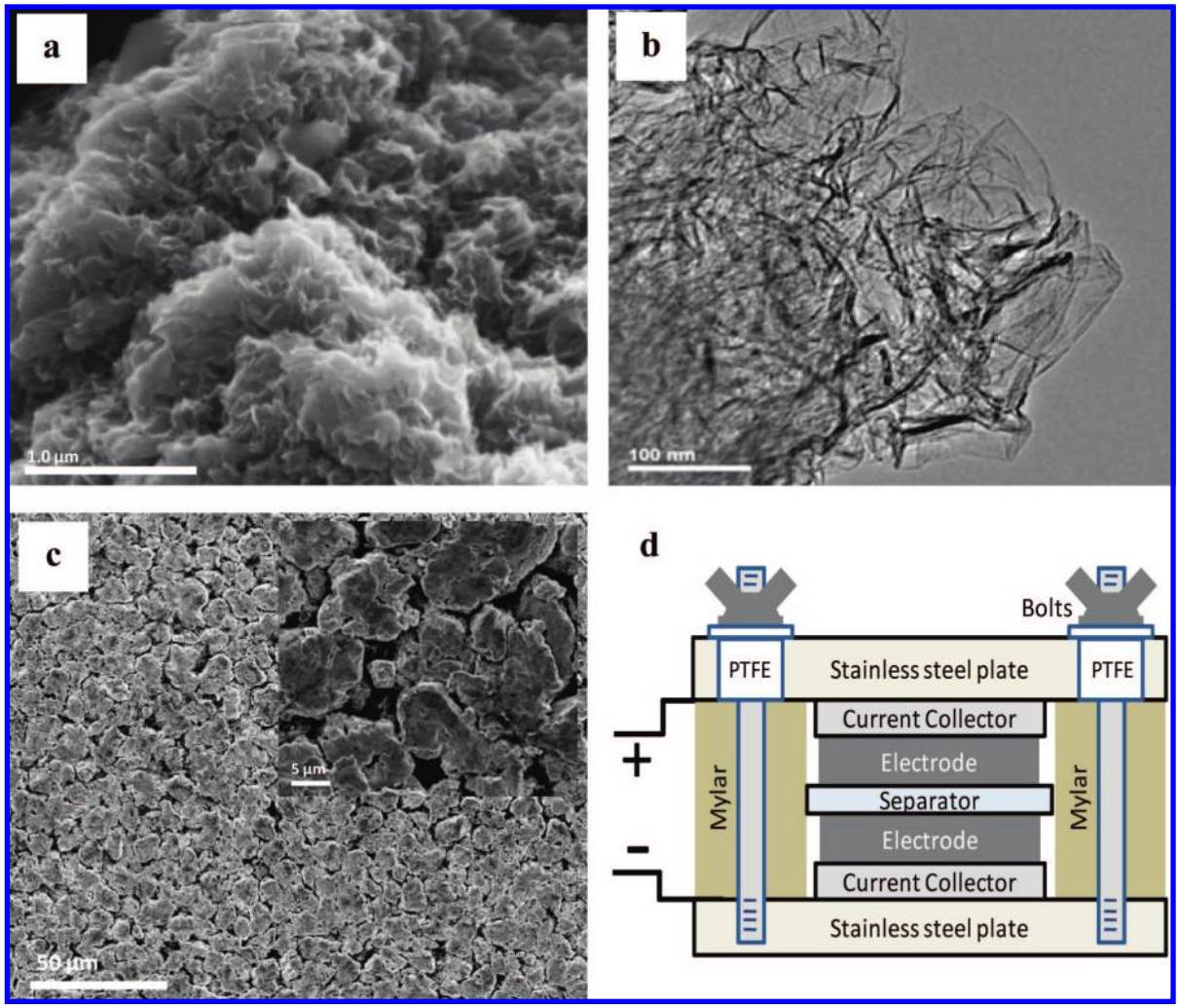

Figure 1. (a) SEM image of CMG particle surface, (b) TEM image showing individual graphene sheets extending from CMG particle surface, (c) low and high (inset) magnification SEM images of CMG particle electrode surface, and (d) schematic of test cell assembly.

materials, commercial electrodes are limited in thickness and usually contain conductive but low surface area additives such as carbon black to enable rapid electrical charge transfer from the cell. The measured conductivity of these CMG materials ($\sim 2 \times 10^2$ S/m) closely approaches that of pristine graphite.[8] The high electrical conductivity of the graphene materials eliminates the need for conductive fillers and allows increased electrode thickness. Increasing the electrode thickness and eliminating additives leads to an improved electrode material to collector/separator ratio, which in turn further increases the energy density of the packaged ultracapacitor.

CMG materials can be synthesized with several methods into various morphologies.[9] They can be kept suspended in solution,[10,11] configured into paperlike materials,[12,13] and incorporated into polymer[6] or glass/ceramic[14] nanocomposites. A form of CMG[8] that could be readily incorporated into ultracapacitor test cell electrodes was used for this study. It was synthesized by means of suspending graphene oxide sheets in water and then reducing them using hydrazine hydrate. During reduction, the individual "graphene" sheets agglomerate into particles approximately 15−25 μm in diameter, as measured using scanning electron microscope (SEM) images. The C/O and C/N atomic ratios determined using elemental analysis by combustion of the CMG powder sample were 11.5 and 23.0, respectively. Figure 1a shows a SEM image of the surface of the CMG agglomerate particles. Figure 1b is a transmission electron microscope (TEM) image that shows individual graphene sheets extending from the outer surface. The images illustrate how both sides of the individual sheets at the surface of the agglomerate are exposed to the electrolyte. The surface area of the CMG agglomerate as measured by the N_2 absorption Brunauer−Emmett−Teller (BET) method is 705 m^2/g. Even though the graphene sheets located within the agglomerated particles may not be accessible by the electrolyte, sheets at the surface can provide an indication of CMG's potential for use in ultracapacitor electrodes.

Electrode material characterization can be performed using either a two or a three-electrode configuration. The two-electrode test cell configuration was used because it provides the most accurate measure of a material's performance for electrochemical capacitors.[15] The CMG particles were formed into electrodes using a polytetrafluoroethylene (PTFE) binder, and a stainless steel test fixture was used for electrical testing of the assembled cell. Figure 1c shows two SEM images (low and high magnification) of the surface of an as prepared

Table 1. Specific Capacitance (F/g) of CMG Material

	galvanostatic discharge (mA)		cyclic voltammogram average (mV/sec)	
electrolyte	10	20	20	40
KOH	135	128	100	107
$TEABF_4$/PC	94	91	82	80
$TEABF_4$/AN	99	95	99	85

electrode. Figure 1d shows a schematic of the two-electrode ultracapacitor test cell and fixture assembly. CMG-based ultracapacitor cells were tested with three different electrolytes commonly used in commercial EDLCs.[1] The electrolytes included an aqueous electrolyte (5.5 M KOH) and two organic electrolyte systems, TEA BF_4 in acetonitrile (AN) solvent and TEA BF_4 in propylene carbonate (PC) solvent.

The performance of the ultracapacitor cells was analyzed using cyclic voltammetry (CV), electrical impedance spectroscopy (EIS), and galvanostatic charge/discharge. The CV curves and galvanostatic charge/discharge were used to calculate the specific capacitance of the CMG electrodes. The specific capacitance using the CV curves was reported by integrating over the full CV curve to determine the average value. The specific capacitance determined from galvanostatic charge/discharge was calculated from the slope (dV/dt) of the discharge curves. Table 1 shows the results of specific capacitance (F/g) for the two methods. The EIS data was analyzed using Nyquist plots. Nyquist plots show the frequency response of the CMG electrode/electrolyte system and are a plot of the imaginary component (Z'') of the impedance against the real component (Z'). Each data point is at a different frequency with the lower left portion of the curve corresponding to the higher frequencies. The cell corresponds more closely to an ideal capacitor the more vertical the curve. The intersection of the curve at the *X*-axis represents the internal or equivalent series resistance (ESR) of the cell which determines the rate the cell can be charged/discharged (power capability). The slope of the 45° portion of the curve is called the Warburg resistance and is a result of the frequency dependence of ion diffusion/transport in the electrolyte.

Although the morphology of the CMG material chosen for this first study is such that only a portion of the graphene sheets (those at the surface of the particles) are exposed to electrolyte, the specific capacitances on the order of 100 F/g that were measured show the graphene material works well with current commercial electrolytes, has good electrical conductivity, and has very promising charge storage capability. The cyclic voltammograms (shown in Figure 2) that were obtained are nearly rectangular in shape indicating good charge propagation within the electrodes. For activated carbon-based electrodes, the CV curve shape and the specific capacitance can significantly degrade as the voltage scan rate is increased.[16] Even at scan rates of 40 mV/sec, the CV curves for the CMG-based electrodes remained rectangular with little variance in specific capacitance. Another indication of good charge propagation is the low variation of specific capacitance for increasing voltage scan rates. Table 2 shows the specific capacitance of CMG electrodes with KOH electrolyte for scan rates varying from 20 to 400 mV/sec. In addition to the low electrical resistance of the CMG material, another possible reason for the insensitivity to varying voltage scan rates is a short and equal diffusion path length of the ions in the electrolyte. This may be due to the electrolyte not penetrating into the particulate thus resulting in only the graphene sheets at the particulate surface being accessed. This could also explain the short Warburg region on the Nyquist plots. Ion diffusion into the interior of the agglomerate would result in greater variations in ion diffusion path lengths and an increased obstruction of ion movement resulting in a much larger Warburg region. The high conductivity of the CMG material also contributes to the low ESR of the cells. The internal cell resistance (real Z' axis from Nyquist plots) was 0.15 Ω (24 kHz), 0.64 Ω (810 kHz), and 0.65 Ω (500 kHz) for KOH, $TEABF_4$/PC, and $TEABF_4$/AN electrolytes, respectively.

The change in specific capacitance with respect to voltage also remains relatively linear at the higher voltages. Test cells with KOH electrolyte were cycled to 1 V, cells with PC were cycled to 2.7 V, and AN were cycled to 2.5 V. The presence of a low percentage of functional groups in the CMG material may contribute to a small amount of pseudocapacitance; however, the relatively linear increase of current with increasing voltage indicates that the charge is primarily nonfaradic in nature.[17] The specific capacitance of KOH at 40 mV/sec scan rate during charging remained almost a constant 116 F/g between 0.1 and 0.9 V. The specific capacitance of the organic electrolyte using AN during discharge at 20 mV/sec was 100 F/g in the range from 1.5 V to fully discharged at 0 V. The specific capacitance of the organic electrolyte using PC during discharge at 20 mV/sec was about 95 F/g in the range from 2.0 V to fully discharged at 0 V.

Chemically modified graphenes with good electrical conductivity and very large (and in principle completely accessible) surface areas, are extremely promising candidates for EDLC ultracapacitors. Our results applying these materials to ultracapacitors show they are compatible with commonly used electrolyte systems. In addition, these CMG materials are based on abundantly available and cost-effective graphite. Ultracapacitors based on these materials could have the cost and performance that would dramatically accelerate their adoption in a wide range of energy storage applications.

Methods. Graphite oxide (GO) was synthesized from natural graphite (SP-1, Bay Carbon, MI) by a modified Hummers method.[17] The graphite oxide (100 mg) was loaded in a 250 mL round-bottom flask and purified water (17.4 MΩ, 100 mL) was then added, yielding an inhomogeneous yellow-brown dispersion. This dispersion was sonicated using a Fisher Scientific FS60 ultrasonic bath cleaner (150 W) until it became clear with no visible particulate matter. Hydrazine monohydrate (1.00 mL, 32.1 mmol, 98% from Sigma Aldrich) was then added, and the suspension was heated in an oil bath at 100 °C under a water-cooled condenser for 24 h over which the reduced graphene oxide sheets gradually precipitated out as a black solid. This product was isolated by filtration over a medium fritted glass funnel, washed copiously with water (5 × 100 mL) and methanol (5 × 100

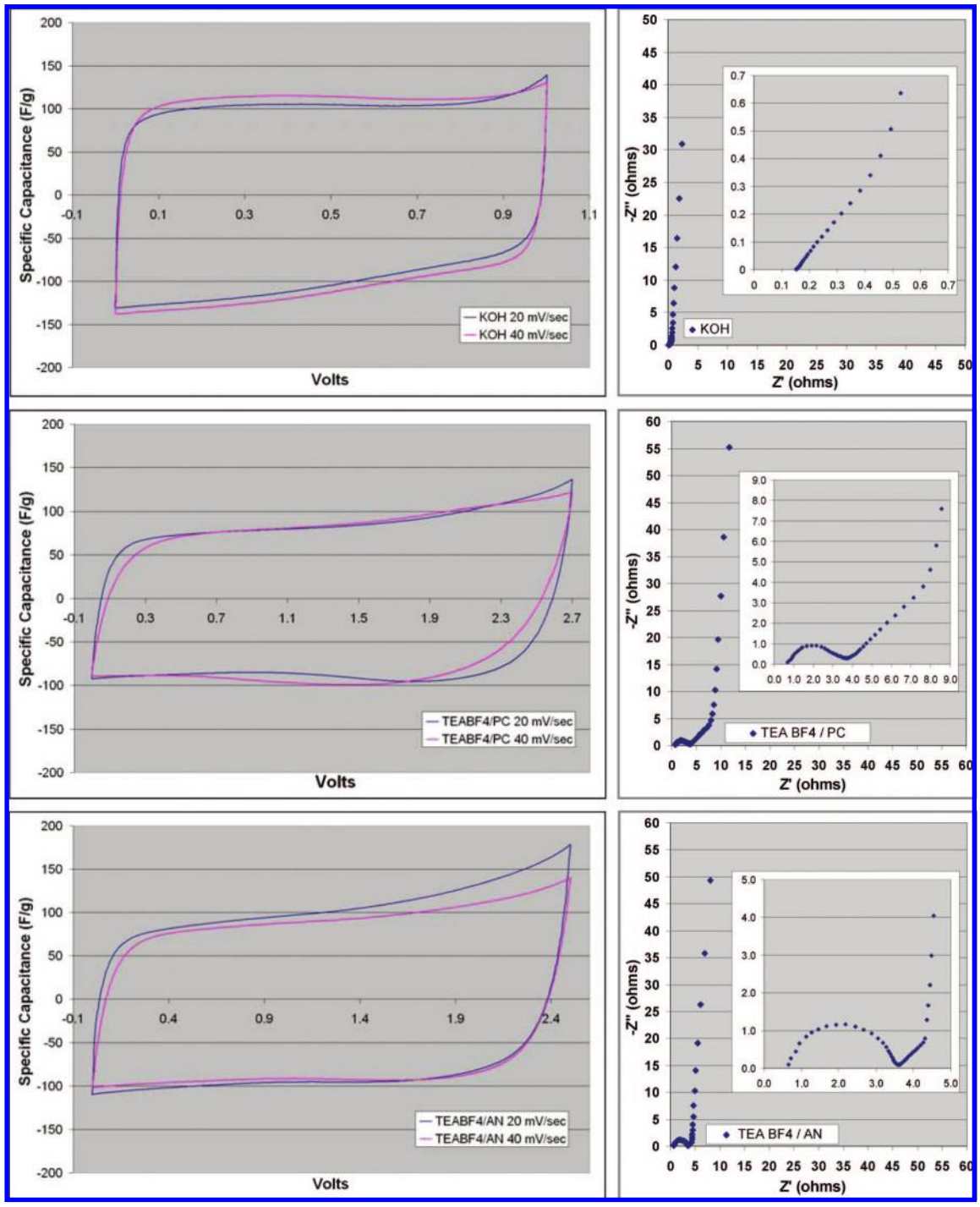

Figure 2. CV (left) and Nyquist (right) plots of CMG material with KOH electrolyte (top), TEA BF_4 in propylene carbonate (middle) and TEA BF_4 in acetonitrile (bottom).

Table 2. Specific Capacitance (F/g) of CMG Material in KOH Electrolyte by Scan Rate (mV/sec)

scan rate (mV/sec)	CV average specific capacitance (F/g)
20	101
40	106
100	102
200	101
300	96
400	97

mL), and dried on the funnel under a continuous air flow through the solid product.

The CMG particles consisting of agglomerated graphene sheets were assembled into electrodes by mixing with 3% by weight polytetrafluoroethylene binder (PTFE 60% dispersion in H_2O, Sigma Aldrich). The mixture was homogenized in an agate mortar, formed into electrodes by rolling the CMG/PTFE mixture into 75 μm thick sheets, and finally by punching out 1.6 cm diameter discs. The nominal weight of an electrode was 0.0075 g. The two electrode test cell assembly is made of two current collectors, two electrodes, and a porous separator (Celgard 3501). The collector material

was from Intelicoat Technologies: a 4 mil conductive vinyl film was used with the aqueous electrolyte and a 0.5 mil aluminum foil with conducting carbon coating was used with the organic electrolytes. The cell assembly was supported in a test fixture consisting of two stainless steel plates fastened together using threaded bolts. Spacers (PET, McMaster Carr) were placed between the SS plates to electrically isolate the plates, provide a hermetic seal, and maintain a consistent, even pressure on the cell.

Aqueous electrolyte was 5.5 M KOH (Fisher). Organic electrolytes were prepared using 1 M tetraethylammonium tetrafluoroborate (TEA BF_4, electrochemical grade >99%, Sigma Aldrich) in acetonitrile (anhydrous, 99.8%, Sigma Aldrich) or in propylene carbonate (anhydrous, 99.7%, Sigma Aldrich). Test cells using organic electrolytes were assembled in a dry nitrogen environment (Atmos glovebag).

CV curves, electrical impedance spectroscopy (EIS), and galvanostatic charge/discharge testing was done with an Eco Chemie Autolab PGSTAT100 potentiostat equipped with the FRA2 frequency response analyzer module and GPES/FRA software. CV curves were scanned at voltage ramp rates of 20 and 40 mV per second. EIS was done using a sinusoidal signal with mean voltage of 0 V and amplitude of 10 mV over a frequency range of 500 000 to 0.01 Hz. Capacitance values were calculated for the CV curves by dividing the current by the voltage scan rate, $C = I/(\mathrm{d}V/\mathrm{d}t)$. Specific capacitance reported is the capacitance for the carbon material of one electrode (specific capacitance = capacitance of single electrode/weight CMG material of single electrode), as per the normal convention. Galvanostatic charge/discharge was done at constant currents of 10 and 20 mA. Capacitance as determined from galvanostatic charge/discharge was measured using $C = I/(\mathrm{d}V/\mathrm{d}t)$ with $\mathrm{d}V/\mathrm{d}t$ calculated from the slope of the discharge curves.

SEM images were obtained with a field emission gun scanning electron microscope (SUPRA 40 VP, Zeiss SMT AG, Oberkochen, Germany). TEM images were taken on a JEOL 2010F. Elemental analysis was performed by Atlantic Microlab, Inc., Norcross, Georgia. BET surface area measurement was done using a Quantachrome Instruments Nova 2000.

Acknowledgment. S.P. was partially supported by a Korea Research Foundation Grant funded by the Korean Government (MOEHRD) (KRF-2006-352-C00055). This work was otherwise supported by a startup package to RSR by The University of Texas at Austin and by the Texas Nanotechnology Research Superiority Initiative (TNRSI)/SWAN. This work made use of EIS facilities at the Center for Nano and Molecular Science and Technology, University of Texas at Austin. We thank S. M. Lipka and C. L. Swartz for helpful discussions. R. Istvan and A. L. Ruoff critically read an initial draft of this manuscript.

References

(1) Conway, B. E. Electrochemical Supercapacitors: Scientific Fundamentals and Technological Applications; Plenum Publishers: New York, 1999.
(2) Kotz, R.; Carlen, M. Principles and applications of electrochemical capacitors. *Electrochim. Acta* **2000**, *45*, 2483–2498.
(3) Burke, A. Ultracapacitors: why, how, and where is the technology. *J. Power Sources* **2000**, *91*, 37–50.
(4) *Basic Research Needs for Electrical Energy Storage: Report of the Basic Energy Sciences Workshop on Electrical Energy Storage*; April 2−4, 2007. Office of Basic Energy Sciences, DOE, July 2007.
(5) Pandolfo, A. G.; Hollenkamp, A. F. Carbon properties and their role in supercapacitors. *J. Power Sources* **2006**, *157*, 11–27.
(6) Stankovich, S.; Dikin, D. A.; Dommett, G. H. B.; Kohlhaas, K. M.; Zimney, E. J.; Stach, E. A.; Piner, R. D.; Nguyen, S. T.; Ruoff, R. S. Graphene-based composite materials. *Nature* **2006**, *442*, 282–286.
(7) Geim, A. K.; Kim, P. Carbon wonderland. *Sci. Am.* **2008**, *298*, 90–97.
(8) Stankovich, S.; Dikin, D. A.; Piner, R. D.; Kohlhaas, K. A.; Kleinhammes, A.; Jia, Y.; Wu, Y.; Nguyen, S. T.; Ruoff, R. S. Synthesis of graphene-based nanosheets via chemical reduction of exfoliated graphite oxide. *Carbon* **2007**, *45*, 1558–1565.
(9) Ruoff, R. Calling all chemists. *Nat. Nanotechnol.* **2008**, *3*, 10–11.
(10) Stankovich, S.; Piner, R. D.; Chen, X. Q.; Wu, N. Q.; Nguyen, S. T.; Ruoff, R. S. Stable aqueous dispersions of graphitic nanoplatelets via the reduction of exfoliated graphite oxide in the presence of poly(sodium 4-styrenesulfonate). *J. Mater. Chem.* **2006**, *16*, 155–158.
(11) Li, D.; Muller, M.; Gilje, S.; Kaner, R.; Wallace, G. Processable aqueous dispersions of graphene nanosheets. *Nat. Nanotechnol.* **2008**, *n/a*, n/a.
(12) Dikin, D. A.; Stankovich, S.; Zimney, E. J.; Piner, R. D.; Dommett, G. H. B.; Evmenenko, G.; Nguyen, S. T.; Ruoff, R. S. Preparation and characterization of graphene oxide paper. *Nature* **2007**, *448*, 457–460.
(13) Park, S.; Lee, K. S.; Bozoklu, G.; Cai, W.; Nguyen, S. T.; Ruoff, R. S. Graphene oxide papers modified by divalent ions - Enhancing mechanical properties via chemical cross-linking. *ACS Nano* **2008**, *2*, 572–578.
(14) Watcharotone, S.; Dikin, D. A.; Stankovich, S.; Piner, R.; Jung, I.; Dommett, G. H. B.; Evmenenko, G.; Wu, S. E.; Chen, S. F.; Liu, C. P.; Nguyen, S. T.; Ruoff, R. S. Graphene-silica composite thin films as transparent conductors. *Nano. Lett.* **2007**, *7*, 1888–1892.
(15) Khomenko, V.; Frackowiak, E.; Beguin, F. Determination of the specific capacitance of conducting polymer/nanotubes composite electrodes using different cell configurations. *Electrochim. Acta* **2005**, *50*, 2499–2506.
(16) Lota, G.; Centeno, T. A.; Frackowiak, E.; Stoeckli, F. Improvement of the structural and chemical properties of a commercial activated carbon for its application in electrochemical capacitors. *Electrochim. Acta* **2008**, *53*, 2210–2216.
(17) Stankovich, S.; Piner, R. D.; Nguyen, S. T.; Ruoff, R. S. Synthesis and exfoliation of isocyanate-treated graphene oxide nanoplatelets. *Carbon* **2006**, *44*, 3342–3347.

NL802558Y